Materials Transfer in Electro-Spark Deposition of TiC_p/Ni Metal-Matrix Composite Coating on Cu Substrate

Experiments indicated the material transferred from the depositing electrode to the substrate by producing one deposition each time, primarily through direct molten-metal to molten-metal contact

BY S. K. TANG, T. C. NGUYEN, AND Y. ZHOU

ABSTRACT

Electro-spark deposition (ESD) is a microwelding process that utilizes short duration of electrical pulses to deposit electrode materials to a metallic substrate. In this paper, the material transferred from the depositing electrode to the substrate was investigated by producing one deposition each time. Titanium carbide particles/nickel metal-matrix composite (TiC_p/Ni MMC) was used as the electrode to coat the copper (Cu) substrate in the static mode and the dynamic mode experiments. The movement of the depositing TiC_p/Ni electrode was strictly controlled in static mode experiments. Meanwhile, in dynamic mode experiments, the electrode movement was governed by a spring mechanism. Phenomenological models were developed to detail the events taking place during a single deposition in static and dynamic modes, respectively. The experimental results indicated that the material transferred between the depositing electrode and the substrate is primarily through direct molten-metal to molten-metal contact.

Introduction

Electro-spark deposition (ESD) is a microwelding process that is capable of depositing wear and corrosion resistance coatings to repair, improve, and extend the service life of the components and tools (Refs. 1–5). Chen et al. (Refs. 6, 7) deposited titanium carbide particles/nickel metal-matrix composite (TiC_p/Ni MMC) coating by the ESD process to extend the electrode life in resistance spot welding. During the coating process, short duration of electrical pulses ranging from a few microseconds to milliseconds are used to deposit the electrode material onto component's surface producing a protective layer. The low net heat input and the ability to form metallurgical bonding of coating to substrate are some of the noticeable advantages of the ESD coating process (Refs. 1–5). However, the materials transfer mechanism from the depositing electrode to the substrate during the ESD process is not well understood. There are several theories to the material transfer mechanism during the ESD process. The first theory suggests that the electrode materials are transferred to the substrate via solid, liquid, or gaseous states (Ref. 8). The second theory proposes that the materials transfer mechanism in the ESD process is similar to short-circuit (Ref. 2), globular or spray transfer modes typically observed in the gas metal arc welding (GMAW) process (Ref. 9). The third theory describes the detachment of molten droplets from the electrode tip and impinging onto the substrate surface (Ref. 10). Limited experimental work has been done on validating the proposed theories. As a result, the objective of this study is to enhance the current understanding to the materials transfer from the depositing electrode to the substrate during the ESD process. To accomplish this task, the ESD process was set up to produce one deposition each time. Based on the experimental observations, phenomenological models will be developed to detail the events taking place during the ESD process. Afterward, multiple ESDs were performed at the same substrate location to document the coating evolution.

S. K. TANG, T. C. NGUYEN (tnguyen@conestogac.on.ca)*, and Y. ZHOU are with Centre for Advanced Materials Joining, University of Waterloo, Waterloo, Ont., Canada. NGUYEN is also with School of Engineering and Information Technology, Conestoga Polytech, Kitchener, Ont., Canada.*

KEYWORDS

Electro-Spark Deposition (ESD)
Titanium Carbide Particles/Nickel Metal-Matrix Composite (TiC_p/Ni MMC)
Copper (Cu) Substrate
Dynamic Deposition Mode

Materials and Experimental Procedure

Materials

In the present study, the depositing electrode material was the TiC_p/Ni MMC. The 6-mm-diameter electrodes were manufactured by sintering TiC particles that were approximately 5 μm in diameter. In this metal matrix composite, nickel (Ni) and molybdenum (Mo) were used as binding agents. The sintered TiC_p/Ni MMC electrode tip was then ground to 1.5 mm diameter for this study.

The substrate used in the present study was a precipitation-strengthened and work-hardened Class 2 copper (Cu) alloy with the C18150 ASTM specification. In the material transfer and coating evolution studies, the Cu substrate was a circular specimen 25.4 mm in diameter and 1.5 mm thick. In the mass gain and loss quantification study, the Cu substrate was cut into 10 × 10 × 0.8 mm rectangular specimens. Prior to any experiment, the Cu substrate was mechanically ground with 320-grit silicon carbide emery paper and rinsed with acetone to obtain a thin and uniform surface oxide layer.

Table 1 shows the nominal chemical composition of the depositing and substrate materials, respectively.

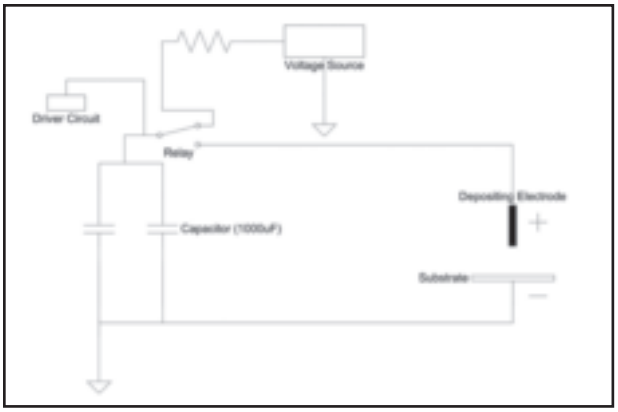

Fig. 1 — Electrical schematic diagram of ESD setup.

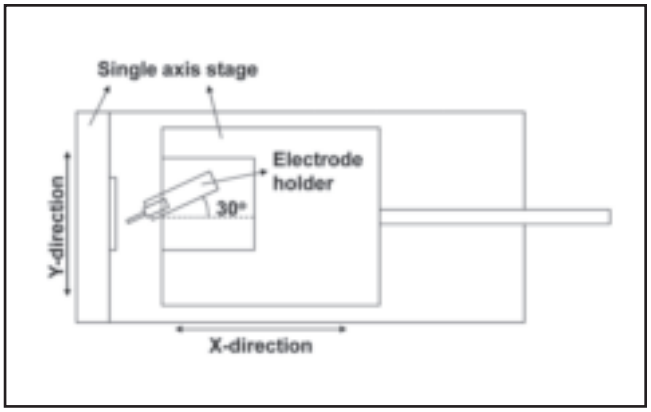

Fig. 2 — Schematic diagram of ESD setup in static deposition mode.

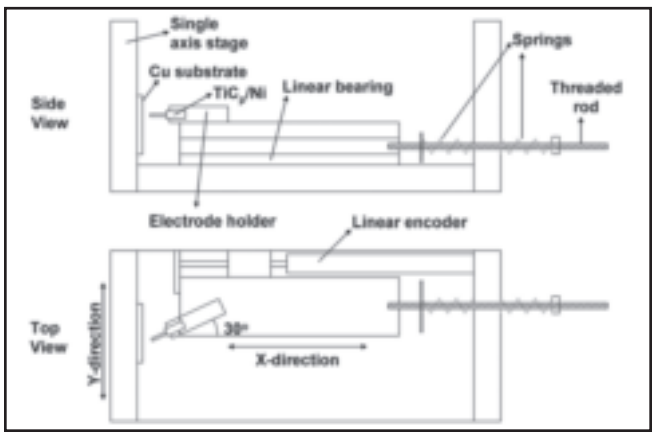

Fig. 3 — Schematic diagram of ESD setup in dynamic deposition mode.

ESD Equipment Setup

The ESD equipment setup used in the present study was designed and built at the Centre of Advanced Materials Joining (CAMJ), University of Waterloo. Figure 1 shows a schematic electrical diagram of the ESD circuit. The ESD circuit consisted of two 1000-μF capacitors, a voltage source, a relay switch, and a computer-controlled driver circuit. The capacitors were used to store and discharge the electrical power during the deposition process. The voltage source was an adjustable constant voltage power supply that could charge up the capacitors to a preset voltage level. The relay was used to control the charge or discharge modes of the ESD circuit. This relay switch was controlled by a computer-controlled driver circuit. In the present study, the ESD circuit was always set to charge mode by default setting of the program. When ready, a command would be inserted into the program to switch the relay into discharge mode.

ESD Coating Studies

In the present study, the TiC_p/Ni coatings were deposited onto Cu substrate by the static and dynamic modes. The movement of the TiC_p/Ni electrode was strictly controlled in static mode experiments. Meanwhile, in dynamic mode experiments, the electrode movement was governed by a spring mechanism. The experiments were conducted using a 35 V charging voltage and 2000 μF capacitance in room-temperature air.

Figure 2 shows the ESD experimental setup used during the static deposition mode testing. The single axis stage was used to hold the Cu substrate that was connected to the negative terminal of the ESD circuit. As illustrated, a single axis stage was utilized to control the movement of the Cu substrate in the Y direction. The electrode holder was used to hold the TiC_p/Ni rod during the deposition process. It was connected to the positive terminal of the ESD circuit and mounted on a second single axis stage. During static mode testing, the TiC_p/Ni MMC electrode was manually moved toward the Cu substrate. The depositing electrode was set at a 30-deg offset angle as shown — Fig. 2. After the TiC_p/Ni electrode was brought to contact with the Cu substrate, the relay switch was turned to discharge mode to create one ESD.

In dynamic deposition mode testing, the TiC_p/Ni electrode was mounted on the spring-loaded mechanical apparatus as shown — Fig. 3. The spring-loaded mechanical apparatus consisted of a single axis stage, an electrode holder mounted on linear bearing, and springs and threaded rod assembly that replaced the second single axis stage. The TiC_p/Ni electrode was initially pushed against Cu substrate. This location was referred to as the zero reference point. Then, the TiC_p/Ni electrode was pulled backward to a location previously set on the springs-threaded rod assembly. At this time, the relay was switched to discharge mode, and the springs-threaded rod assembly was released. The previously compressed spring on one side of the springs-threaded rod assembly sprang forward and brought the TiC_p/Ni electrode into contact with the Cu substrate. This initiated the ESD. While the TiC_p/Ni electrode was moving toward the Cu substrate, a spring on the other side of the springs-threaded rod assembly underwent a compression. This spring would be responsible for moving the TiC_p/Ni electrode back away from the Cu substrate after the discharge, to prevent the TiC_p/Ni electrode from permanently sticking to the Cu substrate. Eventually, the TiC_p/Ni electrode was returned to the original

Table 1 — Nominal Compositions of Depositing and Substrate Materials

Materials	Nominal Composition (wt-%)						
	Ti	Ni	Mo	W	Cu	Cr	Zr
TiC_p/Ni MMC	68.36	15.44	13.40	2.80	—	—	—
C18150 Cu Alloy	—	—	—	—	99.11	0.84	0.05

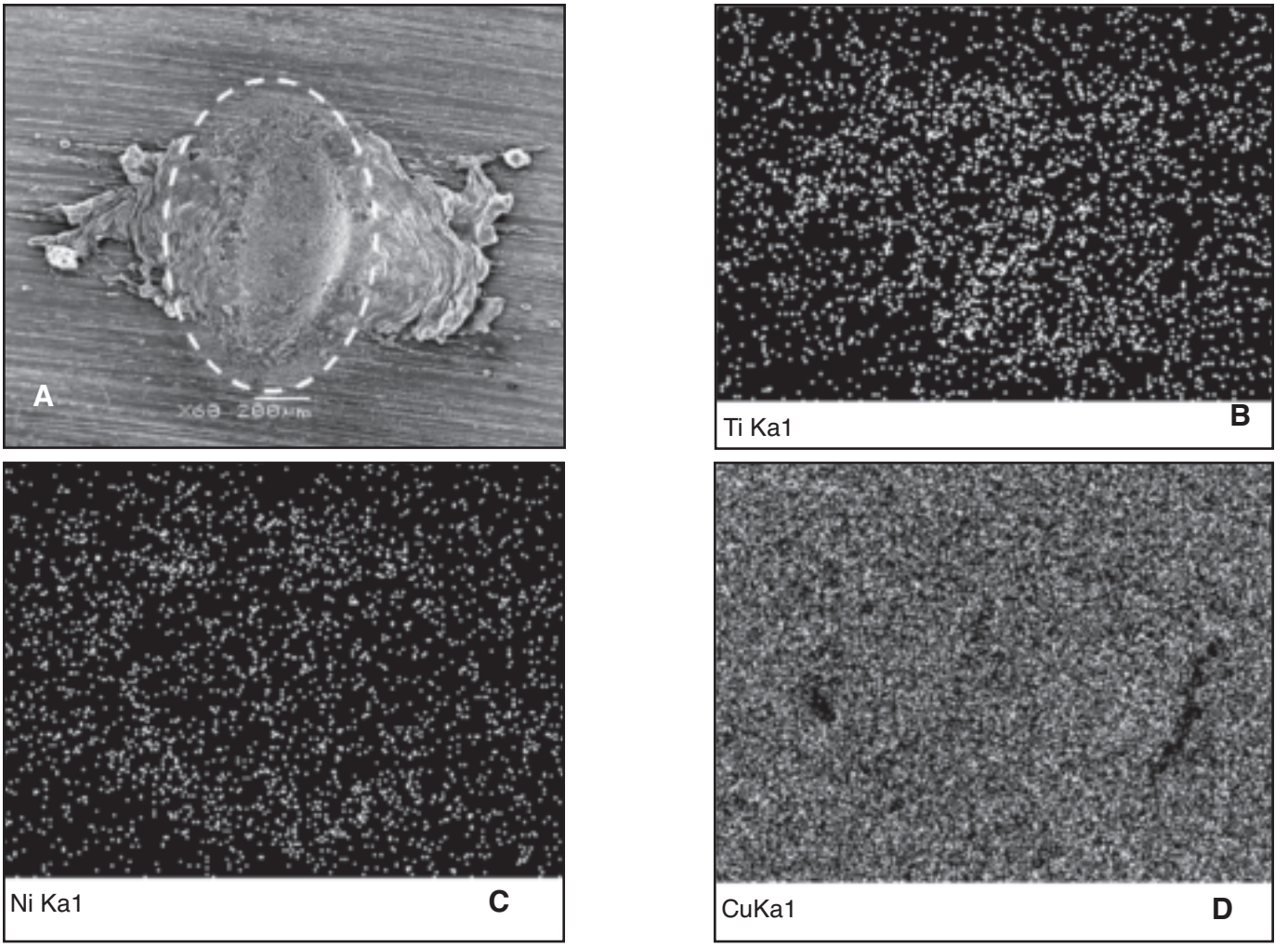

Fig. 4 — SEM image of ESD TiC_p/Ni single deposition. A — Static deposition mode. EDS elemental mapping of B — Ti K_α; C — Ni K_α; D — Cu K_α.

position.

To study the TiC_p/Ni MMC coating evolution, the dynamic mode testing was used repeatedly to create multiple ESD deposits at the same Cu substrate location. To quantify the mass gain and loss on the Cu substrate and TiC_p/Ni electrode, respectively, 20, 40, 60, 80, and 100 ESD deposits were made using the spring-loaded mechanical apparatus. The deposition process was the same as described in the dynamic deposition mode testing. Both the TiC_p/Ni electrode and copper substrate were weighed before and after depositions using a Scientech SM124D analytical balance. In the mass gain and loss study, each testing condition was replicated three times.

Microstructural characterization and chemical analysis were performed using scanning electron microscopy (SEM) and energy-dispersive spectroscopy (EDS) analysis. The surface morphology of the deposition spot was observed under a JEOL JSM 6460 SEM with an attached Oxford Instruments INCA-350 EDS. The EDS elemental mapping and spot analysis were performed to characterize the electrode materials distribution on the ESD spot.

Results

Static Deposition Mode Experiments

Figure 4 shows the SEM image of topographic morphology and accompanying EDS elemental mapping of one ESD of TiC_p/Ni on Cu substrate in static mode. An elliptical crater was created at the center of the deposition area. The molten metal was expelled outward and resolidified on the periphery of the crater. Because the crater was elliptical, the expelled material was not distributed evenly around the periphery. As reported elsewhere (Ref. 11), higher depositing voltages resulted in more molten substrate metal expelled from larger and deeper elliptical crater.

As indicated by the white dashed line in Fig. 4A, a white region surrounding the crater of the deposition is observed. This was possibly caused by the cathode pulverization that is often observed in the reversed polarity gas tungsten arc welding (GTAW) process to remove the surface oxide film on the substrate during welding (Ref. 12). This observation suggests that the ESD process is a self-cleaning process. In addition, the SEM/EDS elemental mapping shows that there is little trace of materials transferred between the TiC_p/Ni electrode and the Cu substrate — Fig. 4B–D.

Figure 5A shows the SEM image of a TiC_p/Ni depositing electrode after performing three single depositions in static mode while Fig. 5B is a close-up SEM image of one of the depositing areas. As clearly shown in Fig. 5B, the solidification structure at the edge of the TiC_p/Ni depositing electrode suggests that melting of the TiC_p/Ni electrode had occurred during the deposition process. Figure 6 shows the variations of current and voltage as functions of time recorded during single deposition in static mode. The voltage level dropped from the

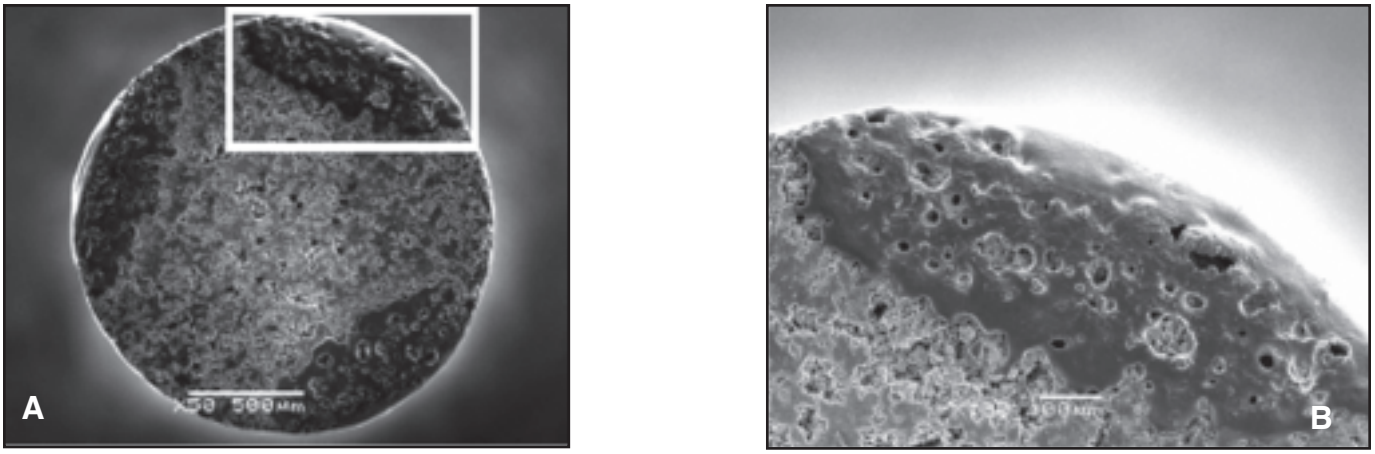

Fig. 5 — SEM images of TiC_p/Ni depositing electrode after three single depositions in static mode. A — The overall image of the electrode end; B — the zoom-in image of the highlighted depositing area.

initial value of 35 to 18 V. Meanwhile, the current suddenly increased to 225 A. After reaching the peak of 225 A, the current rapidly declined back to 0 A, while the voltage was leveled out at 18 V. The voltage and current plot of Fig. 6 illustrates that the capacitors were partially discharged.

Dynamic Deposition Mode Experiments

Figure 7 shows the SEM image of topographic morphology and accompanying EDS elemental mapping of ESD single deposition of TiC_p/Ni onto Cu substrate in dynamic mode. The deposition spot had the same surface appearance as the static mode. An elliptical crater was created at the center of the deposition area, and the expelled molten Cu substrate solidified along the minor axis of the elliptical crater. As in the static mode, a white region surrounding the crater was also observed — Fig. 7A. Unlike the static mode, there was quantitative evidence of TiC_p/Ni material transferred to the Cu substrate as shown on the EDS elemental mappings of Fig. 7B–D. The single deposition spot consisted of the Cu substrate and small amount of TiC and Ni. As mentioned previously, the depositing electrode was composed of TiC particles with Ni as one of the binding agents. Overall, high concentrations of titanium and nickel were found at the center of the deposition crater as illustrated by the chemical analysis — Fig. 8.

Figure 9 shows the SEM and EDS elemental mapping images of the end surface of TiC_p/Ni electrode used in single dynamic deposition experiments. In Fig. 9A, three different melted areas are approximately located at the 10, 1, and 5 o'clock positions, respectively. The 10 o'clock melted area is the area of interest in the subsequent discussion. Meanwhile, the remaining melted areas came from other single deposition experiments. As shown in Fig. 9B, a molten structure was evident at the edge of the TiC_p/Ni depositing electrode. In addition, copper was found at the edge of the molten area on TiC_p/Ni electrode. In fact, SEM/EDS elemental mapping of Fig. 9D shows the presence of copper at both the top and bottom of the depositing area on the TiC_p/Ni electrode. This is a clear evidence of copper pickup during the dynamic deposition process.

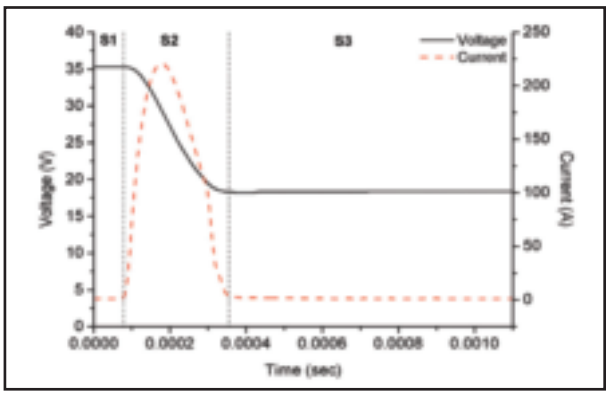

Fig. 6 — Current and voltage waveform of ESD single deposition in static deposition mode.

Figure 10 shows the current, voltage, and displacement as function of time during single deposition in dynamic mode. In this case, the capacitors were completely discharged during the deposition process. The voltage level dropped from 35 to 0 V, and two current peaks were observed. The discharge cycle can be divided into two halves. First, the voltage level dropped from the initial value of 35 to 16 V. Meanwhile, the current suddenly increased to 350 A, and the displacement kept rising. After the current reaching the peak of 350 A, the current rapidly declined to 50 A, and the voltage declined linearly to 13 V. At this stage, the displacement curve reached its peak at 4 μm. In the second half of the discharge cycle, the voltage decreased rapidly from 13 to 1 V. At the same time, the current quickly increased to 225 A, and the displacement declined slowly. After the current reaching the second peak of 225 A, the current rapidly declined to 0 A, and the voltage leveled at 0 V.

ESD Coating Buildup by Multiple Depositions at the Same Spot

In this study, the ESD coating evolution was observed using multiple depositions at the same spot on the Cu substrate. For this part of the study, the applied voltage was set at 35 V. Figure 11A–H shows the SEM topography micrographs of the first eight TiC_p/Ni multisingle depositions on the same spot. Figure 11I–L shows the topography of the TiC_p/Ni coating after 20, 40, 60, and 80 depositions on the same spot, respectively. As illustrated by these figures, the deposition spot was progressively getting bigger, and more TiC_p/Ni material was deposited on the substrate as the number of depositions increased. Initially, the first deposition is identical to the single deposition observed in dynamic mode experiment. An elliptical crater was formed as the substrate's material and surface contaminant were expelled outward from the deposition crater. After the first deposition, the elliptical crater on the Cu substrate contained a mixture of Cu, TiC, and Ni concentrations similar to that observed in Fig. 8. Meanwhile, the TiC_p/Ni electrode was covered by a thin film of resolidified materials as shown in Fig. 9.

As illustrated in Fig. 12A, after three consecutive deposits, the deposition spot was changed from the elliptical crater to

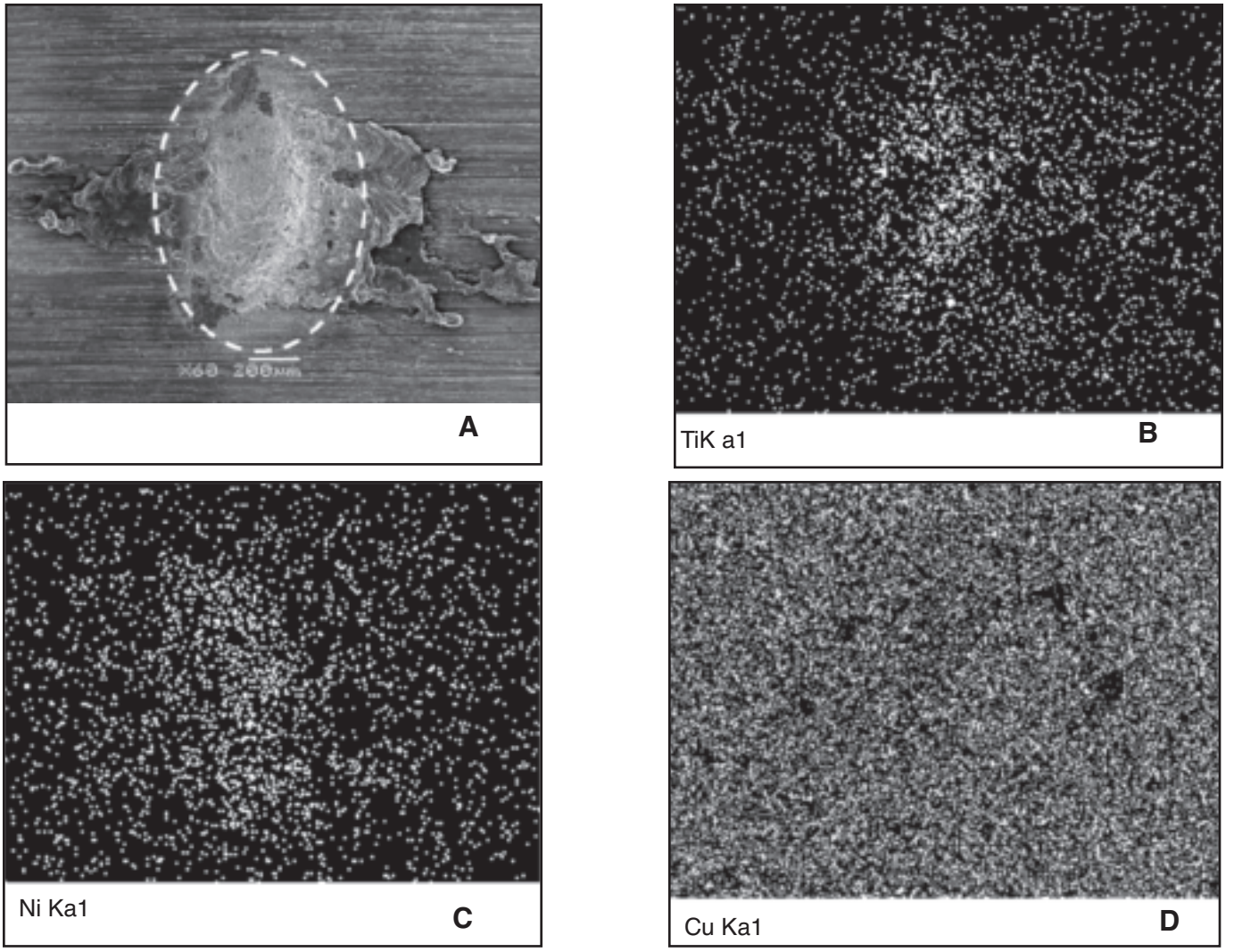

Fig. 7 — SEM image of ESD TiC_p/Ni single deposition. A — Dynamic deposition mode. EDS elemental mapping of B — Ti K_α; C — Ni K_α; D — Cu K_α.

the typical splash appearance of ESD coating (Refs. 8, 10, 13). After further depositions, the coating began to crack as shown in Fig. 12B and C. In Fig. 12D, a dense coating was formed but separated by cracks, and the ESD splash appearance was no longer observed.

Discussion

Phenomenological Models for the Formation of ESD Single Deposition

Based on observations of the surface morphology of Cu substrate, the surface of the TiC_p/Ni electrode, SEM/EDS analysis results and the collected current and voltage data, a model detailing the events taking place during the formation of a single deposition in static mode was developed. Figure 13 shows schematically the phenomenological model of the formation of one deposition in static mode. The model can be divided into three stages. In stage 1 (S1), the TiC_p/Ni electrode was manually brought into contact with the Cu substrate using the single axis stage. There was no further movement after the TiC_p/Ni electrode touched the Cu substrate. During this stage, the relay switch was opened and thus the ESD circuit was still in the charge mode. As a result, as illustrated in Fig. 6, the voltage stayed in the preset level with no current flowing.

The second stage began with the closing of the relay switch to initiate the discharge of the capacitors. At the beginning of stage 2 (S2), current quickly increased as the voltage dropped. At the microscopic level, there are no two surfaces that are completely flat (Ref. 13). When the electrode and the substrate were brought into contact, only the asperities on the two surfaces were actually touched — Fig. 13. As a result, the current was allowed to pass through these local contact points during discharge. The resistance heating (I^2R) at these local contact areas caused melting and vaporizing of the electrode and the substrate materials — Figs. 4, 5. In addition, because of the high current density at these local contact points, a spark was initiated between the electrode and the substrate. The spark expelled the molten Cu substrate forming a crater at the depositing location. The elliptical appearance of the crater was the result of the sharp edge geometry of the electrode and the 30 deg contact angle with the substrate — Fig. 3. The molten metal expulsion removed surface contaminants, thereby improving the overall bonding quality between the substrate and the coating material (Refs. 8, 10, 11, 13). After the molten metal expulsion, a narrow root opening was formed between the electrode and substrate, preventing further discharge of the capacitors in stage 3 (S3).

As observed from Fig. 4, the surface appearance of the deposition spot is different from the observations reported by Liu et al. (Ref. 13). In the latter case, the

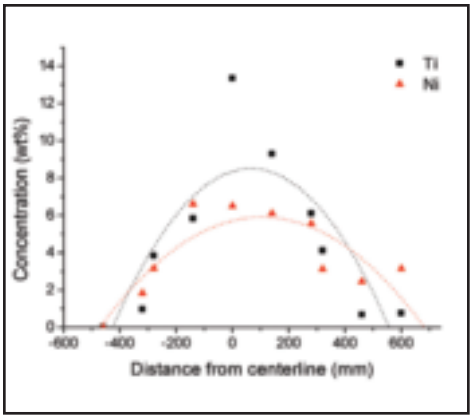

Fig. 8 — The titanium and nickel concentration at different locations across the elliptical crater of an ESD single deposition in dynamic mode.

splash of the coating material on the substrate was reported. This splash appearance of the coating material was the result of the spraying and impinging of molten coating droplets on the substrate surface (Ref. 10). As observed in the present study, the elliptical crater appearance of the deposition crater was formed by the expulsion of molten substrate material. During sparking, a trace of the TiC_p/Ni material was ejected from the electrode tip and then resettled on the surface of the Cu substrate. This could account for the trace evidence of TiC_p/Ni material on the Cu substrate shown in Fig. 4. Based on this experimental observation, the direct spraying of coating electrode material to the substrate did not occur.

In a typical ESD process, the depositing electrode is momentarily stuck to the substrate (Refs. 13, 16). In the present study, however, the static mode did not mimic the ESD process entirely as the TiC_p/Ni electrode movement was restricted. As a result, to further examine the events taken place during a single ESD, a phenomenological model was also developed for the dynamic deposition mode and will be discussed next.

Figure 14 shows the model of the formation of one deposition in dynamic mode. This model can be divided into four stages. In stage 1 (D1), the depositing electrode was traveling toward the substrate as indicated by the increase in the displacement curve in Fig. 10. At this point, no physical contact was made between the electrode and substrate. Thus, there was no current flow at this moment, and the voltage stayed at the preset level of 35 V. In stage 2 (D2–D3), the depositing electrode was brought into contact with the substrate to initiate the discharge. Voltage started to drop rapidly and gave rise to the first current peak. Similar to the static mode, both the electrode and substrate material were rapidly heated and melt at the local contact areas. This led to the formation of melt pool on the substrate and the thin film of molten materials on the electrode surface. After sparking and an ejection of the molten substrate material, there was a momentary root opening between the electrode and substrate. As a result, current started to decline. However, the continuous forward motion of the electrode caused it to contact the substrate again in stage 3 (D4). As evidenced from the displacement curve in Fig. 10, the displacement of the TiC_p/Ni electrode reached its peak in stage 3 (D4).

During stage 3, a thin molten film of both the electrode and substrate materials was formed via a direct molten-metal to molten-metal contact. Consequently, the electrode material was transferred onto the substrate at the points of contact. In addition, during this molten-metal to molten-metal contact, part of the molten Cu substrate material that was ejected to the edge of the crater adhered to the electrode surface as shown — Fig. 9. The capacitors discharged the remaining energy and created the second current peak dur-

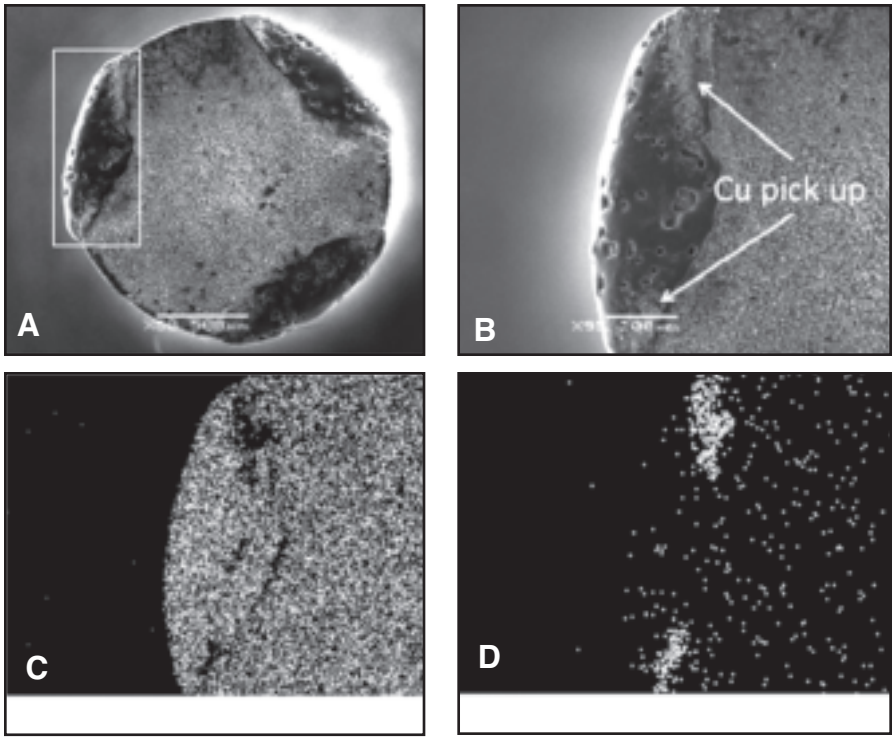

Fig. 9 — SEM images of TiC_p/Ni depositing electrode after single deposition in dynamic deposition mode. A — Overall image; B — zoom-in image; and EDS elemental mapping of C — Ti K_α and D — Cu K_α.

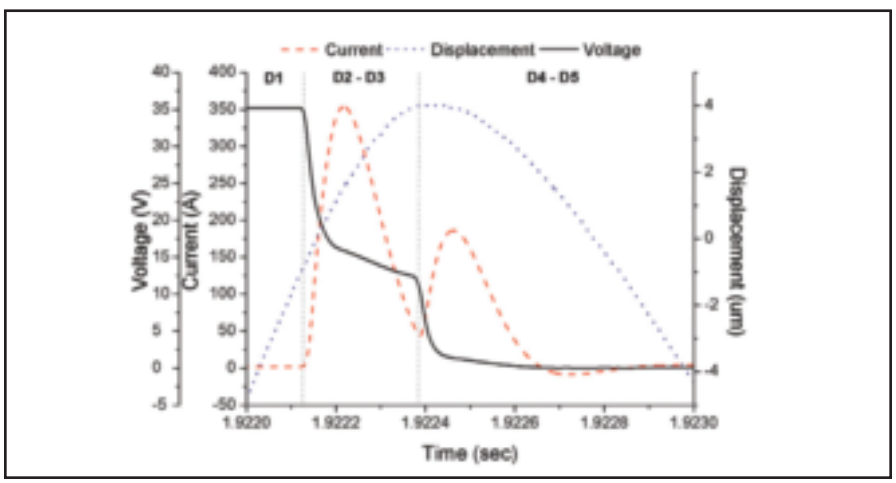

Fig. 10 — Current, voltage, and displacement waveform of ESD single deposition in dynamic deposition mode.

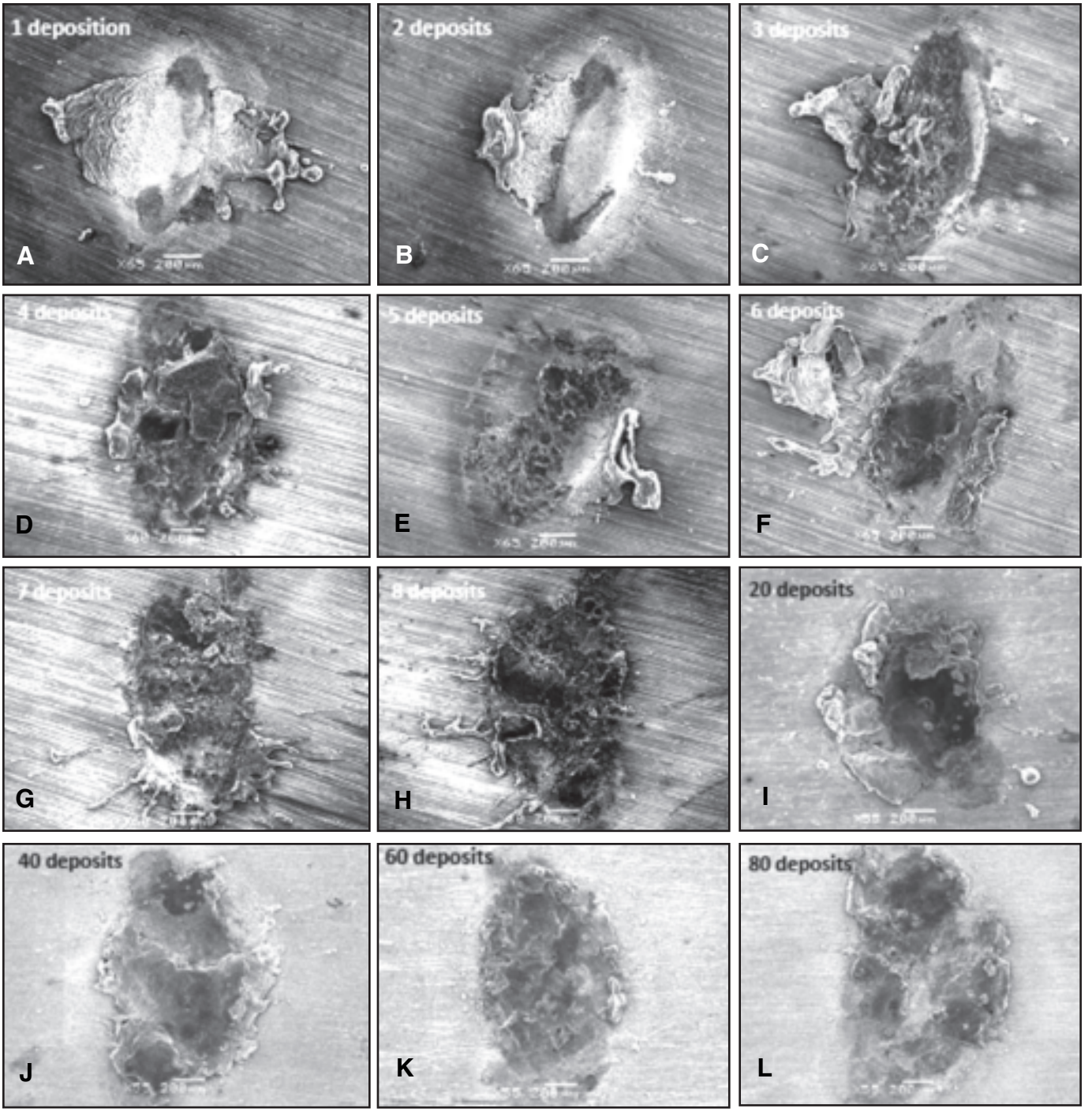

Fig. 11 — SEM micrographs of TiC_p/Ni coating after the following depositions at the same spot: A — 1; B — 2; C — 3; D — 4; E — 5; F — 6; G — 7; H — 8; I — 20; J — 40; K — 60; L — 80.

ing this stage. In the last stage (D5), the TiC_p/Ni electrode was retracted to prevent the local bonding between the Cu substrate and the TiC_p/Ni electrode. The deposited electrode materials were then solidified on the substrate. Finally, the TiC_p/Ni electrode returned to its original position for subsequent depositions.

ESD Coating Buildup on the Substrate

The change of the coating surface appearance during the deposition process was caused by the continuous surface melting and surface erosion of both the TiC_p/Ni electrode and the Cu substrate. After the first deposition, the TiCp/Ni electrode was covered by a thin film of resolidified TiC_p/Ni (see Fig. 9), and the deposition spot on the Cu substrate was covered by a thin layer of the mixture of Cu and TiC_p/Ni. As the deposition progressed, the elliptical crater appearance had disappeared. On subsequent depositions, the contact area between the electrode and the Cu substrate was increased. With a larger contact area, the overall current density was reduced. As a consequence, the amount of molten materials from both the electrode and the Cu substrate were diminished, thereby limiting the amount of metal transferred via molten-metal to molten-metal contact.

After multiple depositions, cracking of the TiC_p/Ni coating was observed. During the deposition process, the molten

TiC_p/Ni was deposited on to the Cu substrate. Because the substrate was a greater heat sink due to the high thermal conductivity of copper, the molten TiC_p/Ni rapidly solidified, thus creating residual tensile thermal stress in the coating (Ref. 4). As the deposition progressed, the buildup of the thermal stress caused more cracks to nucleate and to propagate within the brittle ceramic coating.

Material Transfer between Depositing Electrode and Substrate

As mentioned in the previous section, the ESD coating is the buildup of the coatings by depositing the TiC_p/Ni on the previous deposition spot. Figure 15A and B shows the weight gained by the substrate and the weight lost by the TiC_p/Ni depositing electrode during the ESD process. It is shown that the Cu substrate weight gain increased as the numbers of depositions increased. On the other hand, the TiC_p/Ni depositing electrode lost more weight as the numbers of depositions increased. Interestingly, the TiC_p/Ni weight loss was always greater than the Cu weight gain.

In order to understand the material transfer during the ESD process, the theory of electrode erosion by electrical discharge should be revisited. Various researchers proposed that the electrode erosion by electrical discharge could be taken place in the following three distinct phases: solid, liquid, or vapor (Refs. 17, 18). The solid or vapor phase erosion of the electrode would lead to a net loss while only the liquid phase erosion had a positive net gain on materials transferred during the ESD process.

In solid phase erosion, the eroded solid particles by mechanical impact would not adhere to either the electrode or the substrate surfaces. In vapor phase erosion, the vaporized electrode and substrate materials mostly dissipated to the surrounding. In the static mode experiments of the present study, there was no direct molten-metal to molten-metal contact. Only a small amount of the vaporized materials were condensed and redeposited on the substrate surface. As a result, there was only a trace of materials transferred between the TiC_p/Ni electrode and the Cu substrate in the static mode deposition.

In liquid phase erosion, a portion of the molten electrode and molten substrate were coupled due to the molten-metal to molten-metal contact, and coating was formed on the substrate surface. The importance of the molten-metal to molten-metal contact was clearly illustrated by the comparison between the static and dynamic single deposition testing. In static deposition mode, there was no contact between the electrode and the substrate

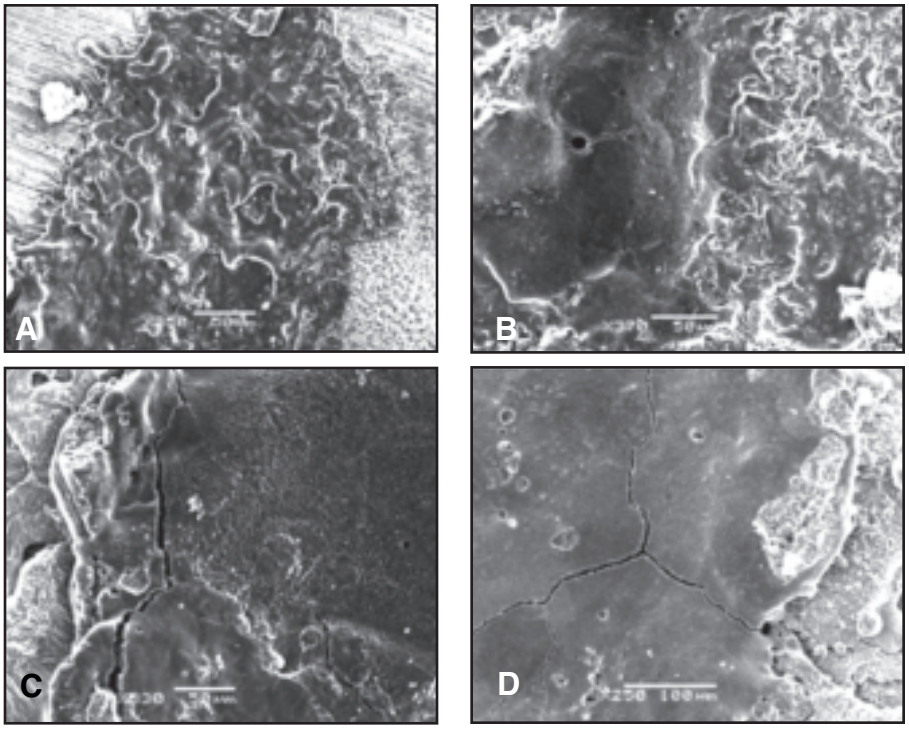

Fig. 12 — SEM micrographs at higher magnifications for the following deposits: A — 3; B — 4; C — 6; D — 60.

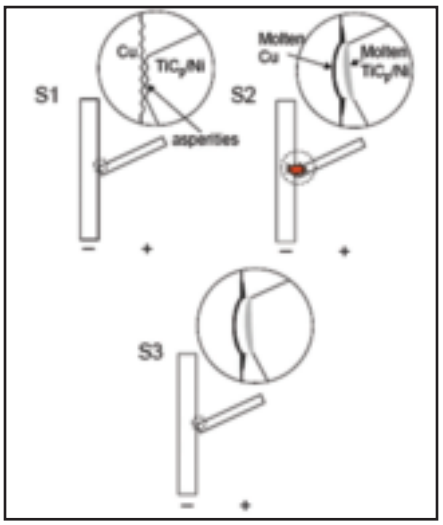

Fig. 13 — Phenomenological model of the formation of ESD single deposition in static deposition mode.

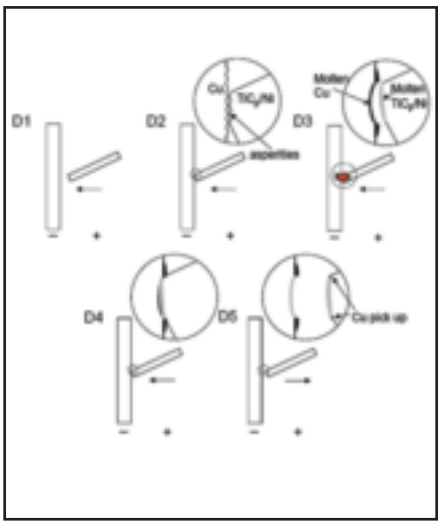

Fig. 14 — Phenomenological model of the formation of ESD single deposition in dynamic deposition mode.

while there was contact in dynamic mode. In the former, there was a trace of electrode materials transferred to the substrate — Fig. 4. On the other hand, in the dynamic mode that had a direct molten-metal to molten-metal contact, the electrode material was clearly present in the Cu substrate crater — Fig. 7. As a result, in this study, the main contribution to the Cu substrate weight gain was obtained through the TiC_p/Ni liquid phase erosion of the depositing electrode. Other phase erosions might also occur on the Cu substrate. The net weight gain of the substrate was then the difference in the weight gain from the TiC_p/Ni deposit minus any copper weight loss due to vapor and solid phase erosions. Meanwhile, the TiC_p/Ni electrode weight loss was mostly caused by liquid phase erosion. In addition, the TiC_p/Ni electrode was also eroded by vapor and perhaps solid phases. In these latter cases, the eroded electrode material did not recondense on the Cu substrate,

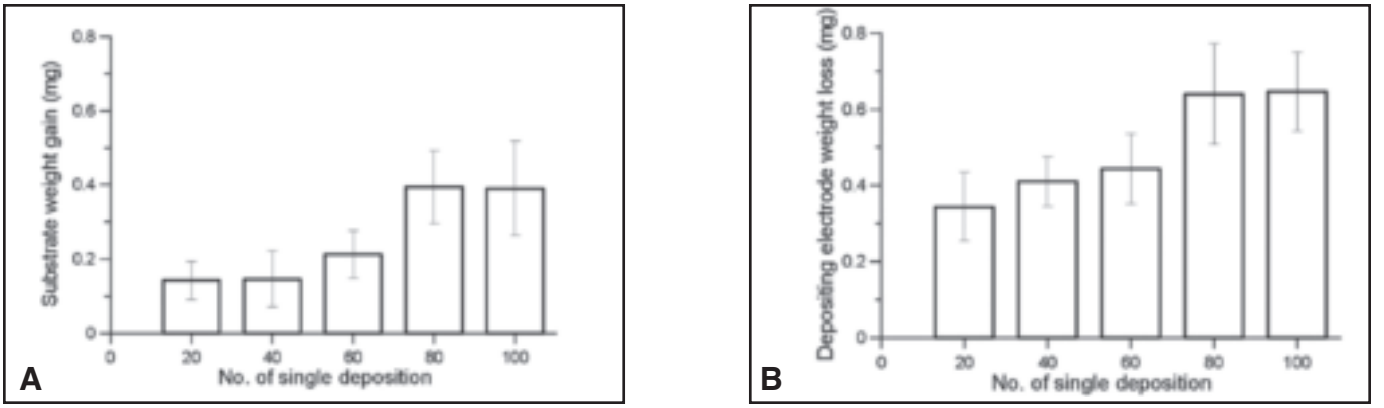

Fig. 15 — A — The weight gained by the Cu substrate; B — the weight lost by the TiC_p/Ni depositing electrode during the ESD process at 35 V.

therefore causing the electrode weight loss to be greater than the substrate weight gain.

According to the above phenomenological model, the materials transfer mechanism between the electrode and substrate was primarily through direct molten-metal to molten-metal contact. This is similar to the hypothesis suggested by Galinov et al. (Ref. 8) who proposed that the molten material on the electrode surface was partly driven away and adhered to the substrate surface. Because the material transfer was through the physical contact between the electrode and the substrate at the center of the deposition crater, the content of the electrode material was expectedly concentrated at the center of the deposition spot as shown — Fig. 8.

In Fig. 15, the amount of weight gained by the Cu substrate and weight lost by the TiC_p/Ni electrode apparently leveled off after 60 depositions. As discussed previously, as the coating was building up, the contact area between the electrode and the substrate was also increased. This resulted in an overall current density reduction. It, therefore, is not surprising that beyond 60 depositions, the amount of weight gained by the Cu substrate and the amount of weight lost by the electrode have reached an upper limit.

Conclusions

In this study, the material transfer mechanism from TiC_p/Ni electrode to Cu substrate during the ESD process was investigated. Once the electrode contacted substrate, an electrical spark was formed due to the extremely high current density at the local contact points. The spark melted and eroded both the substrate and electrode. The crater at the center of the deposition spot was caused by outward expulsion of the molten substrate material. A very narrow root opening was created between the TiC_p/Ni depositing electrode and Cu substrate. At this stage, there was a trace of material transferred between the depositing electrode and substrate. Due to the forward motion of the electrode, the material transfer between the depositing electrode and substrate occurred during the direct molten-metal to molten-metal contact. The TiC_p/Ni electrode weight loss was always greater than the Cu substrate weight gain due to the solid and vapor phase erosion of the electrode. The Cu weight gain was the result of weight gain from the TiC_p/Ni deposit minus any Cu weight loss.

Acknowledgment

The authors would like to thank Natural Sciences and Engineering Research Council (NSERC) of Canada and Huys Industries Ltd. for their financial support.

References

1. Johnson, R. N., and Sheldon, G. L. 1986. Advances in the electrospark deposition coating process. *J. Vac. Sci. Technol. A* 4(6): 2740–2746.

2. Reynolds, J. L., Holdren, R. L., and Brown, L. E. 2003. Electro-spark deposition. *Advanced Materials and Process* 161(3): 35–37.

3. Wang, P. Z., Pan, G. S., Zhou, Y., Qu, J. X., and Shao, H. S. 1997. Accelerated electrospark deposition and the wear behavior of coatings. *Journal of Materials Engineering and Performance* 6(6): 780–784.

4. Parkansky, N., Boxman, R. L., and Goldsmith, S. 1993. Development and application of pulsed-air-arc deposition. *Surf. Coat. Technol.* 61: 268–273.

5. Agarwal, A., Dahotre, N. B., and Sudarshan, T. S. 1999. Evolution of interface in pulsed electrode deposited titanium diboride on copper and steel. *Surf. Eng.* 15(1): 27–32.

6. Chen, Z., and Zhou, Y. 2006. Surface modification of resistance welding electrode by electro-spark deposited composite coatings: Part 1. Coating characterization. *Surf. Coat. Technol.* 201(3-4): 1503–1510.

7. Chen, Z., and Zhou, Y. 2006. Surface modification of resistance welding electrode by electro-spark deposited composite coatings: Part 2. Metallurgical behaviour during welding. *Surf. Coat. Technol.* 201(6): 2419–2430.

8. Galinov, I. V., and Luban, R. B. 1996. Mass transfer trends during electro-spark alloy. *Surf. Coat. Technol.* 79: 9–18.

9. Johnson, R. N. 2002. ElectroSpark deposition: Principles and applications. *Proc. of the Society of Vacuum Coaters 45th Annual Technical Conference*, 87–92.

10. Lesnjak, A., and Tusek, J. 2002. Processes and properties of deposits in electrospark deposition. *Science and Technology of Welding and Joining* 7(6): 391–396.

11. Tang, S. K. 2009. The process fundamentals and parameters of electro-spark deposition. M.A.Sc. thesis, University of Waterloo: 55–58.

12. *Welding Handbook*, Vol. 2, 8th ed., pp. 110–155. 1991. Miami, Fla.: American Welding Society.

13. Liu, J., Wang, R., and Qian, Y. 2005. Formation of a single-pulse electrospark deposition spot. *Surf. Coat. Technol.* 200: 2433–2437.

14. Wilson, R. D., Woodyard, J. R. Sr., and Devletian, J. H. 1993. Capacitor discharge welding: Analysis through ultrahigh-speed photography. *Welding Journal* 72(3): 101s to 160s.

15. Paul, B. K., Wilson, D. D., McDowell, E., and Benjarattananon, J. 2001. Study of weld strength variability for capacitor discharge welding process automation. *Science and Technology of Welding and Joining* 6(2): 109–115.

16. Wang, R., Qian, Y., and Liu, J. 2005. Interface behavior study of WC92-CO8 coating produced by electrospark deposition. *Applied Surface Science* 240: 42–47.

17. Parkansky, N., Beilis, I. I., Rapoport, L., Boxman, R. L., Goldsmith, S., and Rosenberg, Yu. 1998. Anode mass loss during pulsed air arc deposition. *Surf. Coat. Technol.* 108–109: 253–256.

18. Parkansky, N., Beilis, I. I., Rapoport, L., Boxman, R. L., Goldsmith, S., and Rosenberg, Yu. 1998. Electrode erosion and coating properties in pulsed air arc deposition of WC-based hard alloys. *Surf. Coat. Technol.* 105: 130–134.